JOURNAL OF CATALYSIS **160,** 148–154 (1996)
ARTICLE NO. 0134

Distribution of Cations in Mixed Zn–Mn–Al–O Containing Spinels, Model Catalysts for the Reduction of Nitrobenzene to Nitrosobenzene

J. Ziółkowski,* A. M. Maltha,† H. Kist,† E. J. Grootendorst,† H. J. M. de Groot,† and V. Ponec†,[1]

*Institute of Catalysis and Surface Chemistry, Polish Academy of Sciences, ul.Niezapominajek, 30-239 Kraków, Poland; and †Leiden Institute of Chemistry, Gorlaeus Laboratories, Leiden University, P.O. Box 9502, 2300 RA Leiden, The Netherlands

Received August 4, 1994; revised December 13, 1995; accepted January 22, 1996

Nominal $Zn_{1-x}Mn_xAl_2O_4$ ($0 \le x < 1$) solid solutions have been prepared from nitrates in air at 1423 K. $MnAl_2O_4$ was prepared in a flow of 5% H_2/N_2 at 1273 K. All the oxides exhibit the spinel structure with an almost linear variation of the lattice constant with x ($a = 0.80946 + 0.01182x + 0.00497x^2$ [nm]). With the exception of $ZnAl_2O_4$, upon preparation the samples eliminate $0.17x$ of α-alumina, which is compensated by oxidation of some manganese to Mn^{3+}. For charge balance the average valence of Mn should then be 2.11. However, chemical analysis of the sample with $x = 0.5$ shows that there is further oxidation up $Mn^{2.82+}$, which implies that cation vacancies ϕ must be present in the lattice. The above-mentioned chemical analysis, combined with an analysis of the line intensities of the X-ray pattern (Rietveld method, X-ray pattern simulation) and MAS–NMR results (which rule out the presence of Al^{3+} in tetrahedral positions), leads to the formula $(Zn^{2+}_{0.53}Mn^{2+}_{0.09}Mn^{3+}_{0.31}\phi_{0.07})[Mn^{3+}_{0.10}Al^{3+}_{1.84}\phi_{0.05}]O_4$, where parentheses and square brackets denote tetrahedral and octahedral sites, respectively. Intensity analysis combined with X-ray pattern simulations (without chemical analysis) proves that in all the samples $[Mn^{3+}] = 0.17x \pm 0.01$. Assuming that the same oxidation level of Mn exists in all the series, the general formula of the studied solutions should be close to $(Zn^{2+}_{1-x}Mn^{2+}_{0.20x}Mn^{3+}_{0.63}\phi_{0.17x})[Mn^{3+}_{0.17x}Al^{3+}_{2-0.34}\phi_{0.17x}]O_4$.

INTRODUCTION

The analysis presented below is related to catalytic research with spinels of the nominal composition $Zn_{1-x}Mn_xAl_2O_4$ ($0 \le x \le 1$), which appear to be active, selective and stable catalysts for reduction of nitrobenzene to nitrosobenzene (1). Octahedrally sited Mn^{3+} ions are suspected to be the active sites for the reduction of nitrobenzene (1). However, in the ideal spinel $(Zn_{1-x}Mn_x)_{tetr}[Al_2]_{oct}O_4$ there would be only bivalent Mn ions in the tetrahedral positions.

In this article we do not report on the catalytic properties of the Zn–Mn–Al–O spinels, since that information is in another article in this Journal (1). Instead, we concentrate our attention on an analysis of the cation distribution and the Mn oxidation state.

Two introductory remarks have to be placed here:

(i) some of the bivalent-trivalent AB_2O_4 spinels show partially ($0 < t < 1$) or totally ($t = 1$) inverted distribution of cations:

$$(A)[B_2]O_4 \rightarrow (A_{1-t}B_t)[A_tB_{2-t}]O_4 \rightarrow (B)[AB]O_4, \quad [1]$$

where parentheses and square brackets denote the tetrahedral and the octahedral sites, respectively. Rules governing inversion in the two to three spinels have been suggested (2): (a) larger cations prefer the tetrahedral site (size factor), (b) some *d*-electron cations prefer the sites of higher crystal-field stabilization (energy factor), (c) an increase of temperature favors disorder (entropy factor). $ZnAl_2O_4$ is reported (3) to be almost a normal spinel ($t = 0.03$). Although Mn^{2+}; (d^5) is rather large as compared to Al^{3+} (the octahedral ionic radii are 0.083 and 0.053 nm, respectively (4, 5) and MnB_2O_4 and MnB_2S_4 spinels with small B ions show no inversion (3), it was a surprise that $MnAl_2O_4$ was reported to have $t = 0.29$ (3) and only bivalent octahedral Mn ions.

(ii) Eggert and Riedel (6) found that in a particular composition and oxygen pressure range (roughly $0.66 < Cr/(Cr + Fe) < 1$ and $-17 < Lg\ [P_{O_2}\ (bar)] < -6$), Cr_2O_3 is eliminated from $FeCr_2O_4$, and the spinel undergoes oxidation of some iron to Fe^{3+} accompanied by a transfer of Fe^{3+} to the octahedral sites:

$$FeCr_2O_4 + \frac{y}{4(1+y)}O_2 = \frac{1}{1+y}Fe_{1+y}Cr_{2-y}O_4 + \frac{3y}{2(1+y)}Cr_2O_3. \quad [2]$$

By analogy, possibly relevant for Mn-containing aluminates, octahedral Mn^{3+} (d^4) could appear by this mechanism in our spinels.

The combination of these pieces of information concerning inversion in $MnAl_2O_4$ (3), a possible segregation of one

[1] To whom correspondence should be addressed.

0021-9517/96 $18.00

component from the classical AB_2O_4 spinel (6), and the oxidative transfer of ions between tetrahedral and octahedral sites (6) lead us to the hypothesis that octahedral [Mn^{3+} ions could appear in our samples; Mn^{3+} (d^4), in contrast to Mn^{2+} (d^5), has a crystal-field octahedral preference. This idea is further developed in this article.

Let us mention that the same phenomenon (i.e., partial oxidation of manganese to Mn^{3+} and its transfer to octahedra) could have been responsible for an incorrect conclusion with regard to inversion ($t = 0.29$ in $MnAl_2O_4$ (3)).

EXPERIMENTAL

A series of samples of the nominal composition $Zn_{1-x}Mn_xAl_2O_4$ ($0 \le x < 1$) was synthesized by calcination of the stoichiometric mixtures of the *pro analysi* grade metal nitrates in air, first at 1173 K for 20 h and then at 1423 K, again for 20 h. In view of the easy oxidation of Mn^{2+} to Mn^{3+}, $MnAl_2O_4$ ($x = 1$) was produced also from nitrates by a treatment in air at 873 K for 20 h and in a flow of 5% H_2/N_2 at 1273 K for 48 h. With exception of samples indicated as $x = 0.5+$ and $x = 1.0+$, these samples are described in Ref. (1) as series I.

X-ray diffraction patterns were obtained with the automatic Philips diffractometer PW 1050 (Cu$K\alpha$, steps 0.05°/5 s) and treated with the Diffrac program of R. Allman [University of Marburg, Fachbereich Geowissenschaften]. In the two-theta range of 25–70° seven reflections of spinel and eight reflections of α-Al_2O_3 were observed: all reflections were sharp and easily indexable. Lattice constants were calculated with the homemade Lines program [R. A. G. de Graaff (Leiden Institute of Chemistry, The Netherlands)].

As the first approximation, the distribution of cations over the tetrahedral/octahedral sites has been determined by the method proposed by Bertaut (7) and developed by Greenwald *et al.* (8) as described below. The Rietveld method of X-ray pattern simulation has been applied using the DBWS-9006PC program of A. Sakthivel and R. A. Young (School of Physics, Georgia Institute of Technology, Atlanta, GA 30332).

In samples showing free α-alumina, the amount of it was determined by the internal standard method, i.e., by adding weighed amounts of α-Al_2O_3 to the alumina-free $ZnAl_2O_4$ and comparing the intensities of the three strongest and well-separated reflections of α-alumina in the studied samples and in the standards. The error of determination is estimated to vary between 1 and 5% depending on the content of alumina.

The location of Al^{3+} ions in tetrahedral/octahedral sites was determined by ^{27}Al MAS–NMR spectroscopy (Bruker spectrometer) for samples with x equal to 0.5, 0.7, and 1.0 (detectable limit of $(Al)_{tet}$ is 0.007 mol%/mol of spinel). The elemental analysis was done by commercial Microanalytisches Labor Pasher, Remagen, Germany. In their procedure the sample was fused with a mixture of sodium carbonate and sodium borate and dissolved in a HNO_3/HCL mixture: Detection of metals was carried out by inductively coupled argon plasma emission spectroscopy. For independent determination of oxygen, the sample was melted with a Ce/Ni alloy in a graphite capsule at 2273/3273 K under vacuum; oxygen converted into CO was detected by IR spectroscopy.

RESULTS AND DISCUSSION

1. Basic Results

As already mentioned, each of the intended (nominal) $Zn_{1-x}Mn_xAl_2O_4$ ($0 \le x \le 1$) preparations contained mainly the cubic spinel phase and with the exception of $ZnAl_2O_4$ also a small amount of α-alumina, both phases showing sharp and easily indexable reflections.

The determined lattice parameters of the spinels along with the amount of free α-alumina and experimental X-ray reflection intensity ratios $I(400)/I(220)$ and $I(400)/I(224)$, to be used in the Bertaut–Greenwald method (8, 9) described below, are gathered in Table 1 and illustrated in Figs. 1–3.

The lattice constants of $ZnAl_2O_4$ ($x = 0$) and $MnAl_2O_4$ ($x = 1$) are close to the literature values (3); those for the remaining samples vary almost linearly with x ($a = 0.80943 + 0.01182x + 0.00497x^2$ [nm]). Samples prepared as described above contained free alumina; the amount q of

TABLE 1

Properties of the Nominal $Zn_{1-x}Mn_xAl_2O_4$ Spinel Solid Solutions

Sample (x nomin)	Lattice constant (nm)	Excess alumina (mol%)	Intensity ratios (400)/(220) Exp.	(400)/(220) Prelim. calc.[a]	(400)/(224) Exp.	(400)/(224) Prelim. calc.[a]
$ZnAl_2O_4$[b]	0.80860					
0	0.80947(03)	0	0.128	0.083	0.360	0.264
0.2	0.81200(10)	3.4	0.152	0.101	0.470	0.323
0.3	0.81398(07)	5.2	0.160	0.108	0.423	0.348
0.4	0.81498(02)	6.6	0.162	0.122	0.475	0.399
0.5	0.81642(07)	9.9	0.187	0.133	0.516	0.437
0.5+[c]	0.81610(04)	8.4	0.175	0.133	0.534	0.437
0.6	0.81840(10)	9.1	0.196	0.147	0.601	0.485
0.7	0.82046(03)	10.8	0.227	0.164	0.638	0.540
1.0+[c]	0.82546(40)	17.3	0.376	0.222	1.400	0.745
$MnAl_2O_4$[b]	0.82410					

Note. This table presents some corrected values from the set of values in Ref. (1).

[a] Preliminary calculations with DBWS with tentative distribution coefficients, resulting from Eq. [4]. $ZnAl_2O_4$ is considered here as a normal spinel.

[b] Literature data, from Ref. (3).

[c] These samples are marked with + in the figures and do not belong to series I in Ref. (1).

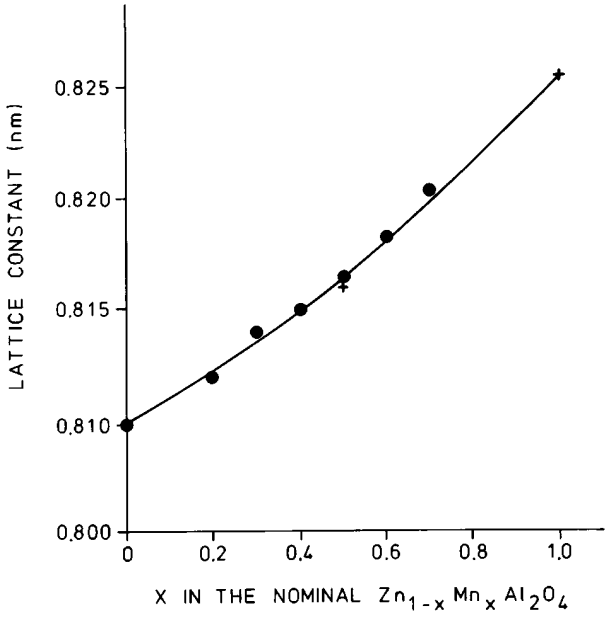

FIG. 1. The almost linear variation of the lattice constants of the nominal $Zn_{1-x}Mn_xAl_2O_4$ spinel solid solutions with the composition x; $a = 0.80946 + 0.01182x + 0.0497x^2$ (nm).

the eliminated α-alumina increases linearly with x, the values being $q = 0.17x$ of Al_2O_3 per mole of the nominal spinel formula. The simple, almost linear relationships ($a = f(x)$, $q = f(x)$), prove that we deal with a consistent series of samples. Also the ratios I(hkl)/I(h′k′l′) vary smoothly along the series (see Table 1 and Fig. 3).

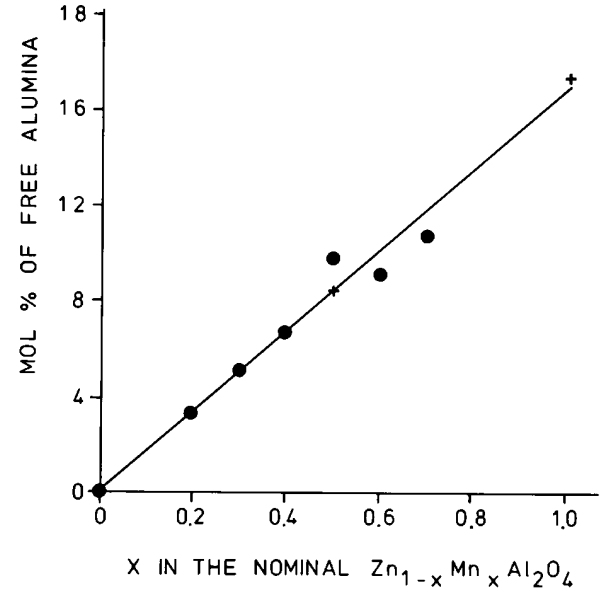

FIG. 2. Mole percent of free α-alumina in the nominal $Zn_{1-x}Mn_xAl_2O_4$ spinel solid solutions as a function of x, equal to the elimination of $0.17x$ Al_2O_3 per mole of the spinel formula.

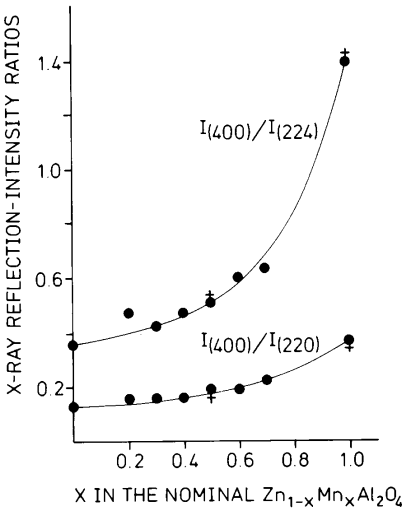

FIG. 3. Intensity ratios I(400)/I(220) and I(400)/I(224) in the X-ray patterns of the nominal $Zn_{1-x}Mn_xAl_2O_4$ spinel solid solutions, as a function of x.

The absence of Al in tetrahedral positions was confirmed by MAS–NMR, as shown in Fig. 4, where solely the pattern of $[Al]_{oct}$ is seen. The tetrahedral pattern would be centered at 54 ppm. The observed elimination of alumina ($q = 0.17x$) points to analogy with the mechanism suggested by Eggert

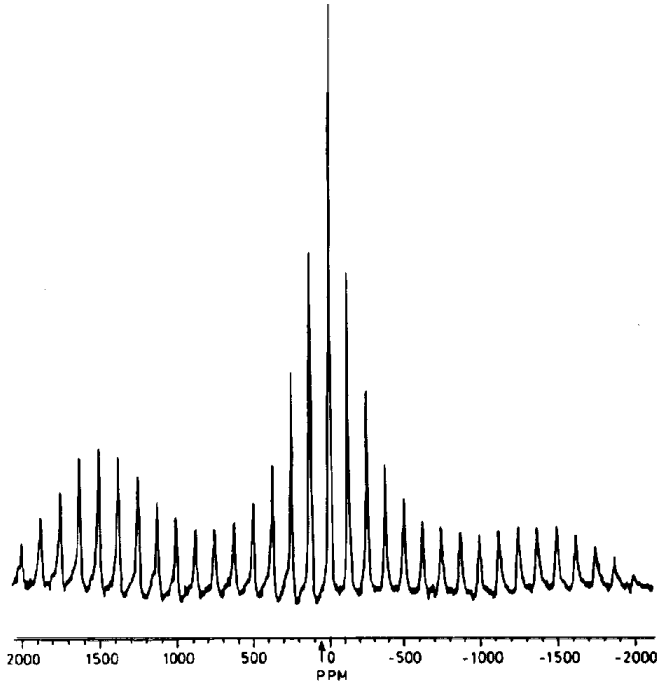

FIG. 4. The ^{27}Al MAS–NMR spectrum of a spinel with nominal composition $Zn_{0.7}Mn_{0.3}Al_2O_4$. The spectrum shows only an octahedrally coordinated Al. The arrow indicates where the tetrahedrally Al signal would be centered (at 54 ppm). The detectable limit of tetrahedral Al (calibration by admixture of a zeolite) is estimated to be 7.10^{-3} mol% with respect to the spinel Al content.

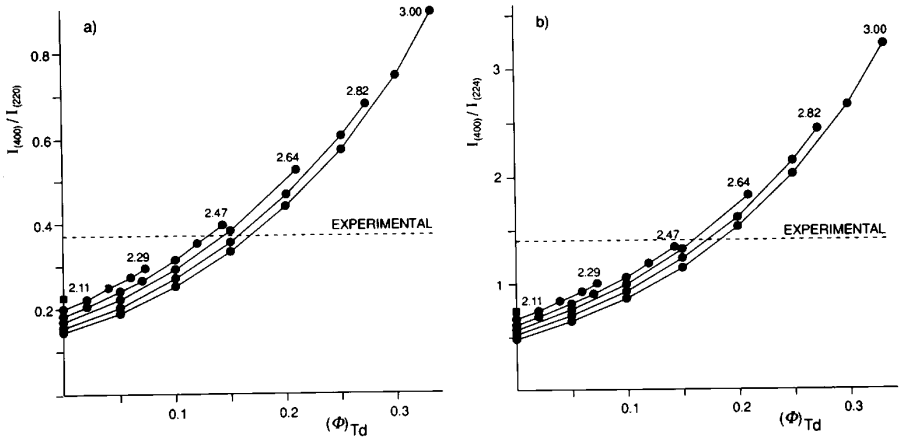

FIG. 5. Calculated $I(400)/I(220)$ (a) and $I(400)/I(224)$ (b) X-ray reflection intensity ratios for $MnAl_2O_4$ as a function of the amount of cation vacancies in the tetrahedral sites. Point at $(\phi)=0$ and curves are labeled with numbers indicating the average valence of Mn. The dotted horizontal lines represent the experimental values of the respective intensity ratios.

and Riedel for $FeCr_2O_4$ (6). By the analogue of this mechanism, Mn^{3+} would appear in octahedral positions and alumina would be displaced out of the spinel.

On the basis of the oxidative-transfer mechanism (6) the spinel formula would be:

$$\left(Zn_a^{2+}Mn_b^{2+}\right)\left[Mn_c^{3+}Al_d^{3+}\right]O_4, \qquad [3]$$

where the parameters a, b, c, d are defined in Eq. [4], describing the reaction of spinel formation,

$$\begin{aligned}(1-x)ZnO + xMnO + Al_2O_3 + z/4O_2 \\ = (1-zx)\left(Zn^{2+}_{(1-x)/(1-zx)}Mn^{2+}_{(x-xz)/(1-zx)}\right) \\ \times \left[Mn^{3+}_{xz/(1-zx)}Al^{3+}_{(2-0.34x)/(1-zx)}\right]O_4 + 0.17xAl_2O_3, \quad [4]\end{aligned}$$

where our $z=0.1133x$ and the average oxidation state of manganese in all the samples of the series is +2.11. However, this picture requires further refinement, as we see below. It is shown that the average valence of Mn must be higher and consequently cation vacancies must be present in the lattice.

2. *Principles of the Bertaut–Greenwald Method (B-G)*

To a first approximation the distribution of ions among the tetrahedral/octahedral sites in spinels can be verified with the method proposed by Bertaut (7) and further developed by Greenwald *et al.* (8). Bertaut noted that the intensities of some X-ray reflections are strongly dependent on the tetrahedral/octahedral cationic site occupation and almost insensitive to the distortions in the cubic close packing of oxygen. Information on cation distribution can be obtained by measuring the intensity ratios $I(400)/I(220)$ and $I(400)/I(224)$ and plotting them as a function of t or of any other parameter characterizing the theoretical (calibration) curves. The experimental data have been obtained using the Rietveld analysis (DBWS-9006PC program). The X-ray scattering factors are proportional to the number of electrons in an atom and the presence in the same structure of atoms with different numbers of electrons makes the determination of cation distribution possible. There is a simple qualitative rule that the higher content of "heavy" atoms in octahedra, the higher $I(400)$ and the lower $I(220)$ and $I(224)$, and consequently, the higher the ratios mentioned above. Examples of the calibration curves are shown in Figs. 5a and 5b. A disadvantage of the method is that it is unable to discriminate between ions of the same (or nearly the same) number of electrons, such as Mn^{2+} and Mn^{3+}. Simplifying assumptions are unavoidable in such a case.

In our case we decided to simplify the problem of occupancy by neglecting the minor impact of the thermal disorder (entropy factor) and by making the following preliminary choice for the distribution of cations (argumentation is indicated in parentheses):

(i) Mn^{2+} as well as Zn^{2+} will be placed always in the tetrahedral sites (large ions, no crystal-field octahedral preference, the error due to the thermal disorder should not exceed 0.003).

(ii) Al^{3+} will always be placed in the octahedral sites (small ion, large strain expected in the case of inversion, no tetrahedral preference, MAS–NMR for the selected samples proved that Al^{3+} is only in octahedral positions).

(iii) Mn^{3+} will be preferentially placed in octahedral sites (octahedral crystal-field stabilization), but its presence in tetrahedra will be admitted. Placing Mn^{3+} and ϕ (vacancies) in both the tetrahedral and octahedral positions should minimize the strain.

3. *Application of the B-G Method to the Zn–Mn–Al–O Spinels in Various Oxidation States of Mn*

The Bertaut–Greenwald method combined with the DBWS program has been applied first to verify the cation distribution according to Eq. [4]. The calculated intensity ratios are collected in Table 1 (entry under prelim. calc.). Ratios calculated in this way are systematically *too small* as compared to the experimental data.

The only way to improve the fit of the experimental and theoretical intensity ratios is (i) to include a higher degree of oxidation of Mn and placing Mn^{3+} (d^4) in octahedra, (ii) to assume the presence of cation vacancies ϕ. Introduction of additional $[Mn^{3+}]$ next to vacancies (ϕ) (we describe it below as ion-vacancy sites swing) permits one to make the octahedra more "heavy" and consequently to increase the calculated intensity ratios used for analysis. Let us consider the consequences of the following reaction (cf. Eqs. [3] and [4]):

$$\begin{aligned} &Zn_a^{2+}Mn_b^{2+}Mn_c^{3+}Al_d^{3+}O_4 + v/2\,O_2 \\ &\quad = \frac{4+v}{4}\left[Zn^{2+}_{4a/(4+v)}Mn^{2+}_{4(b-2v)/(4+v)}\right. \\ &\qquad \left.\times Mn^{3+}_{4(c+2v)/(4+v)}Al^{3+}_{4d/(4+v)}\phi_{3v/(4+v)}\right]O_4. \qquad [5] \end{aligned}$$

Assuming that the highest valence of manganese is +3.00, we deal with the parameter in the region of $v \le b/2$ and $v \le (x-0.1133x^2)/2(1-0.1133x^2)$. We consciously omit the signs indicating the tetrahedral and octahedral location in Eq. [5], since various distributions of Mn^{3+} and vacancies are possible.

In the second approximation the Bertaut–Greenwald method combined with the DBWS program has been applied to verify Eq. [5]. As an example, Figs. 5a and 5b show the changes of $I(400)/I(220)$ and $I(400)/I(224)$ ratios for $MnAl_2O_4$ as a function of $(\phi)_{T/d}$ with the oxidation degrees of Mn ranging from 2.11 to 3.00. The horizontal dotted lines mark the corresponding experimental intensity ratios. It is seen that the best agreement between the experimental and calculated values is reached for average valencies between $Mn^{2.5+}$ and Mn^{3+} (see Table 2). This indicates that the sample $MnAl_2O_4$ shows indeed an ion-vacancy swing (Eq. [5]), but there is a large uncertainity in the distribution coefficients (cf. also Table 2).

It has been mentioned in the introduction that $[Mn^{3+}]$ are suspected (1) to be the active sites for the catalytic reduction of nitrobenzene, for which the studied samples are used as model catalysts. The mere determination of the content of $[Mn^{3+}]$ appears to be much easier than the full determination of the defect structure. Figures 6a and 6b show the same calculated intensity ratios as Figs. 5a and 5b, but now plotted against the octahedral $[Mn^{3+}]$ concentration. All points lie inside a narrow strip between the curves and the uncertainity in determining the $[Mn^{3+}]$ concentration is limited to the horizontal segment of the experimental line, between the curves. Strictly speaking it is slightly larger because the mentioned segments for the $I(400)/I(220)$ and $I(400)/I(224)$ intensity ratios do not coincide exactly. The distribution coefficient of $[Mn^{3+}]$ determined for $MnAl_2O_4$ is 0.195 ± 0.026.

TABLE 2

Selected Examples of Possible Variations in the Zn–Mn–Al–O Spinel Formulas

x	Oxid. state	$(Zn^{2+}$	Mn^{2+}	Mn^{3+}	$\phi)$	$[Mn^{3+}$	Al^{3+}	$\phi]$	O
1.0	2.47	0	0.57	0.29	0.14	0.22	1.78	0	4
	3.00	0	0	0.82	0.18	0.18	1.67	0.15	4
0.7	2.31	0.32	0.51	0.11	0.06	0.12	1.88	0	4
	3.00	0.30	0	0.62	0.08	0.08	1.76	0.16	4
0.5	2.35	0.52	0.35	0.09	0.04	0.09	1.91	0	4
	3.00	0.50	0	0.44	0.06	0.06	1.83	0.10	4
0.3	2.50	0.71	0.15	0.09	0.04	0.07	1.93	0	4
	3.00	0.70	0	0.25	0.05	0.05	1.90	0.05	4

Note. Distribution coefficients corresponding to the lowest and the highest oxidation states of Mn are indicated in Table 2.

It has been verified for all the samples studied ($0 \le x < 1$) that the general form of graphs analogous to Figs. 5 and 6 is the same. On this basis we determined and have gathered in Table 3 the $[Mn^{3+}]$ stoichiometric coefficients, errors in their determination, and estimated ranges of the average valence of manganese in all the samples. Figure 7 shows the most relevant results in the form of a graph. The octahedral

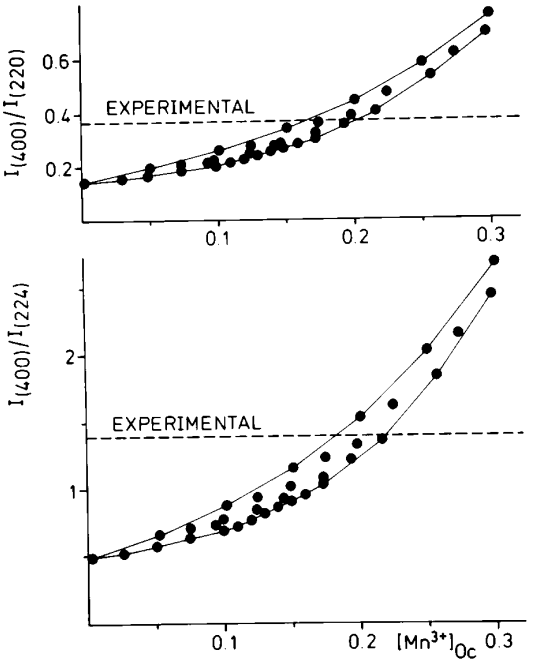

FIG. 6. Intensity data of Fig. 5 drawn as a function of $[Mn^{3+}]_{oct}$.

TABLE 3

Estimated Contents of $[Mn^{3+}]$ in Octahedra in All Samples Studied, Expected Errors in Estimation, and Expected Range in the Oxidation State of Mn

Sample (x)	$[Mn^{3+}]_{oct}$	± Error	Oxidation state range
0.2	0.065	0.005	3.00
0.3	0.067	0.017	2.50 – 3.00
0.4	0.067	0.007	2.35 – 3.00
0.5	0.076	0.014	2.35 – 3.00
0.5 +	0.084	0.014	2.35 – 3.00
0.6	0.093	0.019	2.42 – 3.00
0.7	0.106	0.028	2.31 – 3.00
1.0	0.195	0.026	2.47 – 3.00

$[Mn^{3+}]$ increases almost linearly with x along the series:

$$[Mn^{3+}] = 0.17x\ (\pm 0.01). \qquad [6]$$

The most relevant information for catalysis is thus obtained with a reasonable accuracy. The spinels with a low Mn content show (1) an activity higher than one would expect according to Eq. [6]. Presumably, the surface segregation of Mn^{3+} also plays a role.

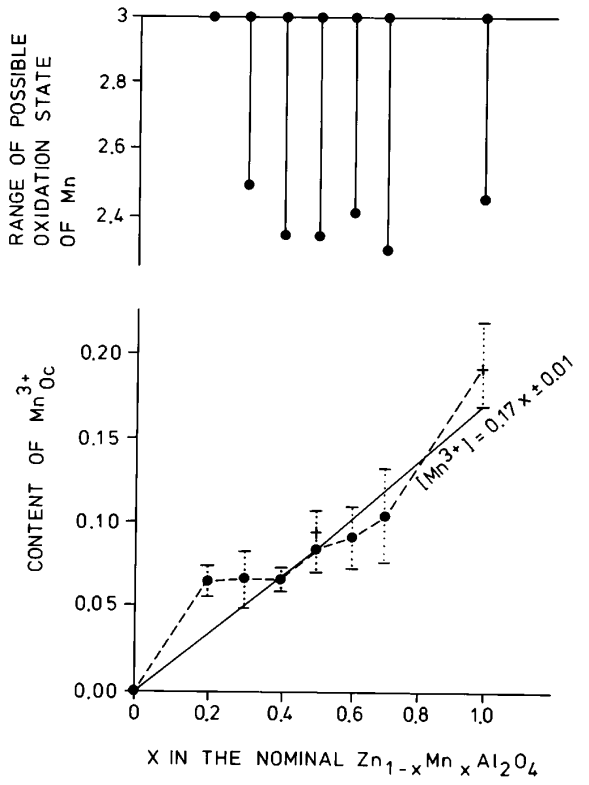

FIG. 7. Estimated content of Mn^{3+} in octahedra as a function of x in the nominal $Zn_{1-x}Mn_xAl_2O_4$ spinels (bottom) and the ranges of possible oxidation states of Mn in the studied samples (top). The octahedral trivalent manganese important for catalysis changes as $[Mn^{3+}] = 0.17x \pm 0.01$.

4. Defect Structure of Zn–Mn–Al–O Spinels

The main purpose of this article was to characterize a series of spinel catalysts used in nitrobenzene deoxygenation and, in particular, to learn whether Mn^{3+} can appear in octahedral positions and, if so, to what extent. This question has been answered. However, it is intriguing to stretch the conclusions as far as possible and to make an attempt to estimate the average valency of manganese and consequently the content of Mn^{3+} and cation vacancies ϕ in both tetrahedral and octahedral sites. To do this, an exact chemical analysis is a necessary prerequisite.

For one sample ($x = 0.5$) an exact chemical analysis has been performed and the average Mn valence determined was +2.82. Comparison of the experimental and DBWS-simulated diffraction intensity ratios shows the best fit for

$$\left(Zn^{2+}_{0.53}Mn^{2+}_{0.09}Mn^{3+}_{0.31}\phi_{0.07}\right)\left[Mn^{3+}_{0.10}Al^{3+}_{1.84}\phi_{0.05}\right]O_4 \qquad [7]$$

with an estimated error of coefficients of 0.03. If we assume that the average valence of Mn is 2.82 through the whole series, the following formula fits the results:

$$\left(Zn^{2}_{1-x}Mn^{2}_{0.20x}Mn^{3}_{0.63x}\phi_{0.17x}\right)\left[Mn^{3}_{0.17x}Al^{3}_{2-0.34x}\phi_{0.17x}\right]O_4. \qquad [8]$$

In addition to the experiments described above some other series of samples have been prepared. The *I** series (1) prepared with different thermal treatment (873 K/20 h and 1323 K/20 h) had about twice as much free alumina as the former series. Although the overall picture was qualitatively very similar, the kinetic factor seems to be responsible for the lower yield of spinel achieved with this preparation. A C-series was prepared from mixtures of amorphous citrates (9), a procedure that ensures very good mixing of components. With this series the final treatment was 1173 K/24 h and 1423 K/12 h in air. These samples showed only traces or absence of free crystalline alumina. This means that the defective Zn–Mn–Al–O spinels may exist in a wide range of compositions and the defect structure described in this article cannot be straightforwardly generalized.

CONCLUSIONS

Free α-alumina is eliminated during the preparation of the nominal $Zn_{1-x}Mn_xAl_2O_4$ ($0 \le x \le 1$) phases (applied here). The remaining material oxidizes and forms solid solutions with a defective spinel structure containing Mn^{3+} and cation vacancies ϕ. We deal here with the (i) oxidative transfer on Mn^{3+} into the octahedral sites and with (ii) tetrahedral/octahedral ion-vacancy swing. The average oxidation state of Mn is above 2.4 and rather close to 2.8. The suggested formula for the catalysts used (1) is therefore:

$$\left(Zn^{2+}_{1-x}Mn^{2+}_{0.20x}Mn^{3+}_{0.63x}\phi_{0.17x}\right)\left[Mn^{3+}_{0.17x}Al^{3+}_{2-0.34x}\phi_{0.17x}\right]O_4. \qquad [9]$$

The lattice parameters of these solutions and the $[Mn^{3+}]_{oct}$ content increase smoothly along the series of samples.

ACKNOWLEDGMENT

This work has been supported by the Netherlands Organisation for Scientific Research (NWO).

REFERENCES

1. Maltha, A., Kist, H. F., Brunet, B., Ziółkowski, J., Onishi, H., Iwasawa, Y., and Ponec, V., *J. Catal.* **149**, 356 (1994).
2. O'Neil, H. S. C., and Navrotsky, A., *Amer. Mineralog.* **68**, 181 (1983).
3. Hill, R. J., Craig, J. R., and Gibbs, G. V., *Phys. Chem. Minerals* **4**, 317 (1979).
4. Shannon, R. D., *Acta Crystallogr., Sect. A* **32**, 751 (1976).
5. Ziółkowski, J., *J. Solid State Chem.* **57**, 269 (1985).
6. Eggert, A., and Riedel, E., *Z. Naturforsch. B.* **46**, 653 (1991).
7. Bertaut, F., *C. R. Acad. Sci. Paris* **230**, 213 (1950).
8. Greenwald, S., Pickart, S. J., and Grannis, F. H., *J. Chem. Phys.* **22**, 1597 (1954).
9. Ziółkowski, J., Krupa, K., and Mocala, K., *J. Solid State Chem.* **48**, 376 (1983).